Novel Compact Dual Bandstop Filter Using Radial Stub

Prashant Kumar Singh, Anjini Kumar Tiwary

Abstract – **This work presents a novel compact dual bandstop filter (DBSF) using planar modified radial stub connected in shunt with 50 Ω microstrip line. The simulation results of the DBSF filter demonstrates good dual wideband bandstop filter (BSF) characteristics with 3 dB stopband fractional bandwidth of 65.42 % and 34.23 % at f_1 = 2.4 GHz and f_2 = 5.2 GHz resonating frequencies respectively. The insertion loss and return loss of more than 30 dB and less than 1 dB respectively at both resonating frequencies in the stop bands is also depicted. The proposed filter offers an upper passband response extended up to 10 GHz and a very compact size of 13.4 × 13.4 mm^2 = 179.56 mm^2. To validate the feasibility of the proposed design, few bandstop filters are analyzed, designed and the final proposed structure is fabricated and tested. The experimental results agree well with the simulation results.**

Keywords – **Radial stub filter, bandstop filter, dual band filter, wireless local area network (WLAN).**

I. Introduction

The demand of dual band or multiband systems is tremendously increasing in the modern wireless communication. The problem of spurious responses or interferences from active devices such as harmonics and intermodulations may be encountered in the multiband system. Bandstop filter [1] rejects unwanted signals such as harmonic and spurious signals and allows desired signal to pass through. Active devices, such as high power amplifiers and mixers, utilize single DBSF to remove or suppress the double sideband spectrum, reduce circuit size and reduce cost. In the past few years several techniques have been reported for designing of DBSFs. The dual stopband performance and compact size are attained simultaneously by using the stepped impedance resonators (SIRs) [2-3], but the SIRs are hardly used where frequency ratio (f_2 / f_1) is less than 2. Dual-band bandstop filters using open-circuited stub-loaded resonators are presented in [4]. Compact dual-wideband bandstop filter are designed in [5-6] using open coupled lines and the transversal signal-interaction concept. The low frequency ratio can be achieved by using open stubs and transversal signal interaction concept at the cost of increased complexity in structure and mathematical analysis. A coupled-line stub is proposed for the design of a novel dual band compact BSF [7]. However, due to presence of coupled-line structure, the two stopbands are narrow.

Prashant Kumar Singh and Anjini Kumar Tiwary are with the Department of Electronics and Communication Engineering, Birla Institute of Technology, Mesra, Ranchi, 835215, Jharkhand, India, E-mailc: prashantkrsingh@bitmesra.ac.in, aktiwary@bitmesra.ac.in

A dual-band bandstop filter is designed using dual-mode loop resonator and a cross-coupled capacitor [8] in order to achieve size reduction and a wide rejection bandwidth, but use of lumped elements tend to increase the complexity as well as cost. The defected ground structures [DGSs] are also used to design the DBSFs [9-10]. An intentional defect on the ground plane is employed in DGS which provides band rejection characteristic due to the resonance property at the cost of back radiation and crosstalk. Radiation can be suppressed by using the shield, which results in extra cost. A planar radial configuration can be used to design DBSF instead of DGS, open stub, coupled lines, lumped element or SIRs to minimize the problems of radiation, complexity, stopband bandwidth, cost and frequency ratio. Due to the use of planar structure the radiation problem is eliminated. A planar circuit approach based on the field expansion in terms of resonant modes has been used to characterize a radial-line stub. Radial-line stubs have intrinsic wide stopband characteristic and found to work better than low impedance rectangular stubs when an accurate localization of a zero-point impedance is needed [11].

A novel miniaturized DBSF is proposed in this paper. Here, compactness is achieved by embedding a radial stub within slotted radial stub. The proposed structure does not employ any lumped element, hence the cost is reduced. The proposed structure has several advantages such as compact size, simple structure, low cost, easier fabrication, easier mathematical analysis and wide stopband (3 dB stopband fractional bandwidth (FBW) of 65.42 % at f_1 = 2.4 GHz and 34.23 % at f_2 = 5.2 GHz resonating frequency respectively). The proposed filter has improved upper passband extending up to 10 GHz along with good passband and stopband performances.

II. Design and Simulation Results

The radial stub (RS) provides a low impedance level at well specified insertion points in a wide frequency band. The conventional microstrip radial stub as shown in Fig. 1(a), can be analyzed as a series combination of an inductor and a capacitor as shown in Fig. 1(b) and their value of input impedance (Z_{in}), inductance (L_{rs}) and capacitance (C_{rs}) can be calculated [12] as:

$$Z_{in} \cong -j\frac{120\pi h\beta}{\theta_r\sqrt{\varepsilon_{eff}}}\left(\ln\frac{r_i}{r_o}+\frac{1}{2}+\frac{2}{(\beta r_o)^2}\right) \quad (1)$$

$$L_{rs} = \frac{120\pi h}{\theta_r c}\left[\ln\frac{r_o}{r_i}-\frac{1}{2}\right] \quad (2)$$

$$C_{rs} = \frac{\theta_r r_o^2 \varepsilon_{eff}}{240\pi hc} \tag{3}$$

where, h is dielectric thickness, β is phase constant, θ_r is spanning angle in radian, c is speed of light, ε_{eff} is effective dielectric constant, r_i is inner radius of radial stub and r_o is outer radius of radial stub.

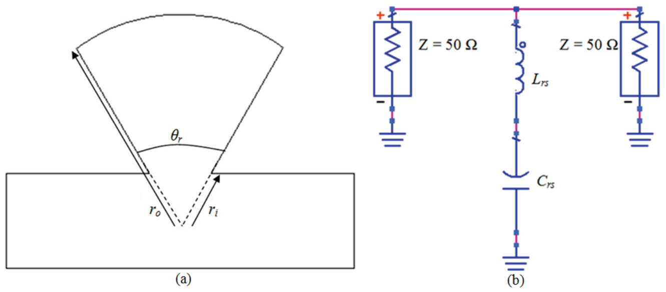

Fig. 1. Bandstop filter and its equivalent circuit model. (a) Radial stub connected in shunt with 50 Ω microstrip line, (b) Equivalent circuit

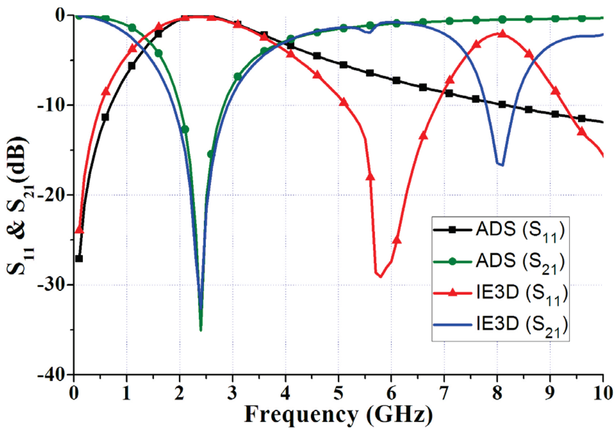

Fig. 2. Simulated results of lumped circuit and microstrip radial structure $f_r = 2.4$ GHz

Using the design equations [11,13-14], the parameters for the conventional microstrip radial resonator for 2.4 GHz resonating frequency (f_r) are obtained as $r_o = 16$ mm, $r_i = 3.5$ mm and $\theta_r = 60^\circ$. For the chosen parameters, the values of inductance and capacitance of lumped equivalent circuit are obtained as $L_{rs1} = 1.6$ nH and $C_{rs1} = 2.8$ pF. All microstrip filter configurations are designed over the substrate which is low cost FR-4 glass epoxy substrate with dielectric constant of 4.4, thickness 1.56 mm and loss tangent 0.016. The microstrip configuration is simulated using IE3D, full wave method of moments (MoM) based simulation software by Zeland. The lumped equivalent circuits are simulated using ADS2009 (Advanced Design System 2009) by Agilent Technologies. The S-parameter characteristics obtained for both lumped and microstrip circuits are compared in Fig. 2. The S_{21} parameter of microstrip circuit differs from the equivalent one in higher frequency range after 6.5 GHz due to the generation of harmonic at 8 GHz. However, the S_{11} characteristics differ after 4 GHz, since the equivalent lumped circuit model may be beyond the constraint conditions in the high-frequency range where the electric length of microstrip lines may be larger than a quarter-wave length and the high-order parasitic effects become dominant. The insertion loss and return loss for microstrip circuit at 2.4 GHz resonating frequency are -32.5 dB and -0.14 dB respectively.

To obtain a stopband at 5.2 GHz, another microstrip radial resonator is designed for 5.2 GHz resonating frequency. The calculated parameter for this is $r_o = 6.5$ mm, $r_i = 1$ mm and $\theta_r = 40^\circ$. The inductance and capacitance values are $L_{rs2} = 3.45$ nH and $C_{rs2} = 0.275$ pF respectively. The S-parameter characteristics of the microstrip structure and equivalent circuits are shown in Fig. 3.

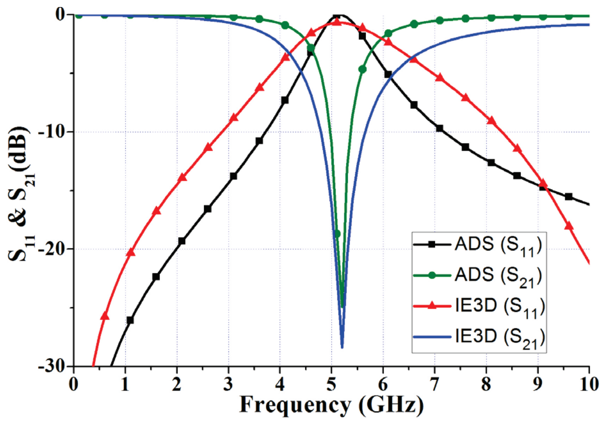

Fig. 3. Simulated results of lumped circuit and microstrip radial structure for $f_r = 5.2$ GHz

Next combining these two radial stub configurations, a dual bandstop filter is designed by connecting these two radial stubs back to back in shunt with 50 Ω line as shown in Fig. 4 to obtain the two stopbands at 2.4 GHz and 5.2 GHz resonating frequencies.

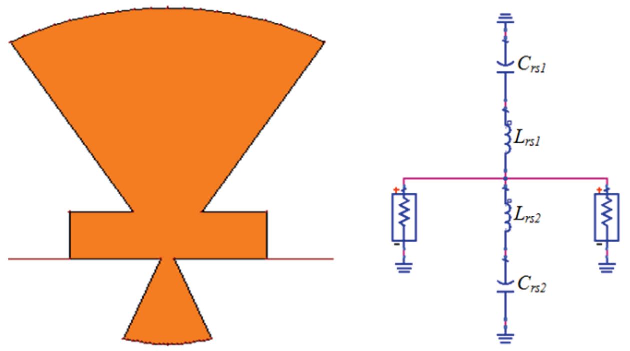

Fig. 4. Dual bandstop filter and its equivalent circuit model

The overall dimension of the structure shown in Fig. 4 is $16 \times 21.5\ mm^2 = 344\ mm^2$. The S- parameters of this dual bandstop filter are shown in Fig. 5. The insertion loss and return loss at 2.4 GHz are obtained as -32.2 dB and -0.16 dB respectively. At 5.2 GHz the insertion and return losses are -40.2 dB and -0.93 dB respectively. One more stopband at 8.5 GHz can be seen in the figure, which can be attributed to the effect of generation of harmonic due to the radial structure for 2.4 GHz resonating frequency as shown in Fig. 2. The two stopbands at 2.4 GHz and 5.2 GHz resonating frequencies can be controlled or shifted to desired location by varying the three parameters of radial structure r_o, r_i and θ_r according to the design equations. However, the stopband at 8.5 GHz is not controllable, which has resulted due to harmonic response of the filter.

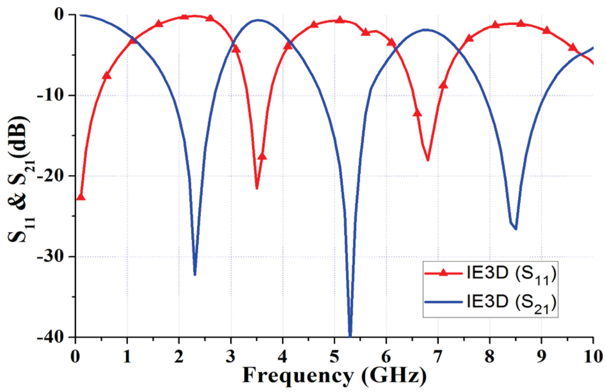

Fig. 5. Simulated result of microstrip dual bandstop filter

Further, in this dual bandstop filter, a radial slot with $r_{o,slot}$ = 8.5 mm, $r_{i,slot}$ = 2.3 mm and $\alpha = 60^o$ is etched in the upper radial stub which is responsible for the stopband at 2.4 GHz resonating frequency as shown in Fig. 6 without altering all other parameters. The stopband at 2.4 GHz is shifted to 1.8 GHz and stopband at 5.2 GHz remains same. In slotted radial structure, the section with dimension $w_1 \times (r_{o,slot} - r_{i,slot})$ works as high impedance inductor (L) of simple straight stub and the upper radial portion with r_o = 16 mm, r_i = 9.5 mm and $\theta = 60^\circ$ works as capacitor (C_{rs1}). As the slot is near to the narrow end of the radial stub, capacitance decreases by very low value, while inductance increases significantly due to the high impedance line. Therefore, the resonating frequency gets shifted towards the lower frequency range. To obtain the stopband at 2.4 GHz, one method is to reduce the outer radius, r_o, of the radial stub to decrease the capacitance. By reducing the outer radius, the overall size of the dual bandstop filter can also be reduced.

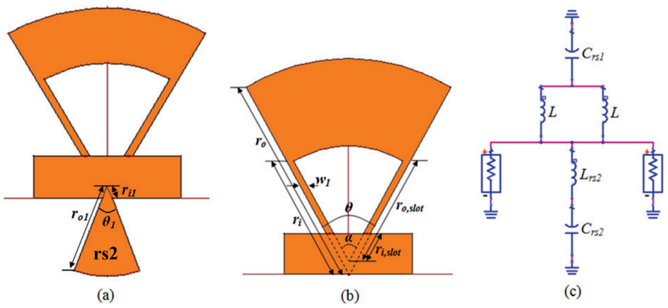

Fig. 6. Slotted radial structure and its equivalent circuit (a) Slotted dual bandstop filter, (b) Slotted section of (a), (c) Equivalent circuit of (a)

To achieve the stopband at 2.4 GHz and 5.2 GHz in slotted radial dual bandstop filter, the dimension of the smaller radial structure is same as is designed for 5.2 GHz which is r_{o1} = 6.5 mm, r_{i1} = 1 mm, $\theta_1 = 40^o$ and the dimension of upper slotted radial structure is r_o = 13.4 mm, r_i = 9.5 mm, $\theta = 60^o$, $r_{o,slot}$ = 8.5 mm, $r_{i,slot}$ = 2.3 mm, $\alpha = 60^o$ and w_1 = 0.58 mm. The overall dimension of the slotted radial dual bandstop filter is 13.4 × 18.9 mm^2 = 253.26 mm^2. A comparative S-parameter characteristics for both unslotted and slotted dual bandstop filters are shown in Fig. 7 and the comparison table with parameters for these two structures is shown in Table I. With size reduction the slotted structure gives good stopband and passband characteristics up to 10 GHz. The uncontrolled harmonic at 8.5 GHz in unslotted filter is suppressed in slotted configuration and the two stopbands can be fully controlled by changing the dimension of the slotted dual bandstop filter.

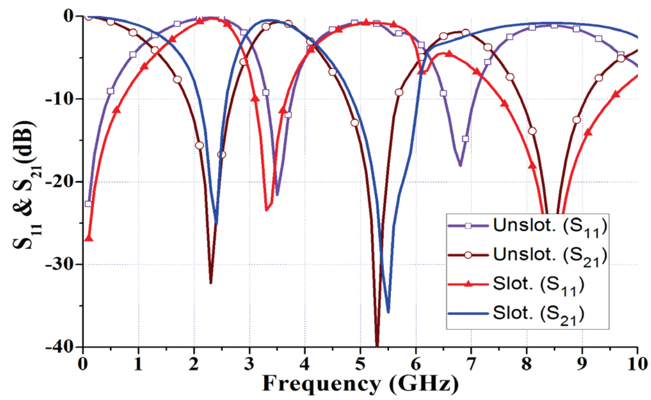

Fig. 7. Simulated results of unslotted and slotted dual bandstop filter

TABLE I
COMPARISON TABLE FOR DUAL BANDSTOP FILTER (DBSF)

Parameters	Without slot		With slot	
Resonating Frequency	2.4 GHz	5.2 GHz	2.4 GHz	5.2 GHz
Insertion Loss	-32.2 dB	-40.2 dB	-25 dB	-35.3 dB
Return Loss	-0.16 dB	-0.93 dB	-0.3 dB	-0.9 dB
-3 dB stopband B.W.	1.9 GHz	2.3 GHz	1.35 GHz	2.45 GHz
Size	344 mm^2		253.26 mm^2	
Overall size reduction as compared to unslotted structure is 26.37 %				

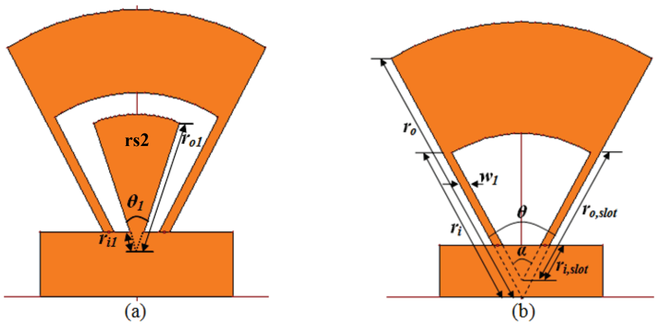

Fig. 8. (a) Embedded radial dual bandstop filter, (b) Slotted section of (a), r_{o1} = 6.5 mm, r_{i1} = 1 mm, $\theta_1 = 40^o$, r_o = 13.4 mm, r_i = 9.5 mm, $\theta = 60^o$, $r_{o,slot}$ = 8.5 mm, $r_{i,slot}$ = 2.3 mm, $\alpha = 60^o$ and w_1 = 0.58 mm

Further, compactness can be achieved by embedding the smaller radial structure within the slotted section of the upper radial structure. All the dimensions of radial and slotted radial stubs in embedded radial DBSF are same as in slotted dual bandstop filter. The embedded radial dual bandstop filter also provides good stopband and passband response. Along with the compactness, the uncontrollable harmonic also gets suppressed. The embedded radial dual bandstop filter configuration is shown in Fig. 8(a), its S-parameter characteristics are shown in Fig. 9 and the comparison table for unslotted and embedded structure is shown in Table II. The final proposed structure has overall dimension of 13.4 × 13.4 mm^2 = 179.56 mm^2.

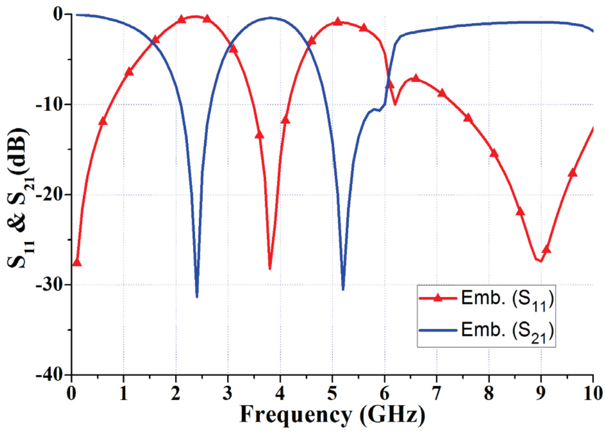

Fig. 9. Simulation result of embedded radial dual bandstop filter

TABLE II
COMPARISON TABLE FOR UNSLOTTED AND EMBEDDED FILTER

Parameters	Unslotted DBSF		Embedded DBSF	
Resonating Frequency	2.4 GHz	5.2 GHz	2.4 GHz	5.2 GHz
Insertion Loss	-32.2 dB	-40.2 dB	-31.2 dB	-30.1 dB
Return Loss	-0.16 dB	-0.93 dB	-0.24 dB	-0.9 dB
-3 dB stopband B.W.	1.9 GHz	2.3 GHz	1.57 GHz	1.78 GHz
Size	344 mm^2		179.56 mm^2	
Overall size reduction as compared to unslotted one is 47.8 %				

III. NETWORK ANALYSIS OF DUAL BANDSTOP FILTER

The proposed model of DBSF with its equivalent circuit is shown in Fig. 10. Here two resonating paths are used. First path is composed of Z_1, Z_2 and $Z_3 = Z_1$ which implies slotted radial section and provides stopband at lower resonating frequency and second path comprises of one shunt radial section with impedance Z_4 which gives a second stopband at higher resonating frequency. In the equivalent circuit interconnection capacitances are neglected. The radial section with impedance Z_2 (~18 Ω) works as a capacitor (C_{rs1}), since its impedance is low. The analysis is performed by employing ABCD parameter of the circuit and then extracting the S-parameters from the ABCD parameter.

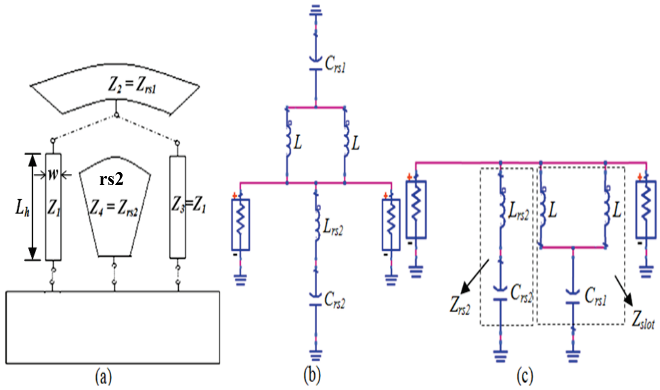

Fig. 10. (a) Proposed model of DBSF, (b) Its equivalent circuit, (c) Simplification of equivalent circuit

The impedances shown in Fig. 10(c) Z_{slot} and Z_{rs2} are calculated as:

$$Z_{slot} = \frac{j\omega L \times j\omega L}{j\omega L + j\omega L} + \left(\frac{1}{j\omega C_{rs1}}\right) = j\omega\left(\frac{L}{2}\right) + \left(\frac{1}{j\omega C_{rs1}}\right) \quad (4)$$

$$Z_{rs2} = j\omega L_{rs2} + \left(\frac{1}{j\omega C_{rs2}}\right) \quad (5)$$

The values of C_{rs1}, C_{rs2} and L_{rs2} are capacitances and inductance of the radial stubs shown by impedances Z_2 and Z_4 respectively. These can be calculated by using Eqs. (2) and (3). Here, ω is the angular frequency and L is the inductance of each rectangular section of slotted radial stub shown by impedances Z_1 and Z_3. The inductance (L) of the rectangular stub can be calculated as [15]:

$$L = \frac{Z_h \sin\left(\beta L_h\right)}{\omega} \quad (6)$$

where Z_h is the characteristic impedance of the rectangular section and L_h is the length of the rectangular section which is equal to $(r_{o,slot} - r_{i,slot})$.

The ABCD parameter for shunt connection is given by [16]:

$$A = 1 \quad (7)$$

$$B = 0 \quad (8)$$

$$C = \frac{1}{Z} \quad (9)$$

$$D = 1 \quad (10)$$

Hence the ABCD matrix for slotted section and radial section is given as:

$$\begin{bmatrix} A & B \\ C & D \end{bmatrix}_{slot} = \begin{bmatrix} 1 & 0 \\ \frac{1}{Z_{slot}} & 1 \end{bmatrix} \quad (11)$$

$$\begin{bmatrix} A & B \\ C & D \end{bmatrix}_{rs2} = \begin{bmatrix} 1 & 0 \\ \frac{1}{Z_{rs2}} & 1 \end{bmatrix} \quad (12)$$

Further the ABCD matrix of complete structure can be calculated as:

$$\begin{bmatrix} A & B \\ C & D \end{bmatrix} = \begin{bmatrix} A & B \\ C & D \end{bmatrix}_{slot} \times \begin{bmatrix} A & B \\ C & D \end{bmatrix}_{rs2} \quad (13)$$

The S_{11} and S_{21} in terms of ABCD with $Z_o = 50\ \Omega$ can be written as [16]:

$$S_{11} = \frac{A + \left(\frac{B}{Z_o}\right) - CZ_o - D}{A + \left(\frac{B}{Z_o}\right) + CZ_o + D} \quad (14)$$

$$S_{21} = \frac{2}{A + \left(\frac{B}{Z_o}\right) + CZ_o + D} \quad (15)$$

From the equivalent circuit, it is clear that there is two resonance condition with $Z_{slot} = 0$ and $Z_{rs2} = 0$, which provides DBSF. By using these two conditions the resonant frequencies can be calculated as:

$$f_1 = f_{r,slot} = \frac{1}{2\pi}\sqrt{\frac{2}{LC_{rs1}}} \quad (16)$$

$$f_2 = f_{r,rs2} = \frac{1}{2\pi}\sqrt{\frac{1}{L_{rs2}C_{rs2}}} \quad (17)$$

Therefore, the first resonant frequency depends on two parameters L and C_{rs1}. From Eq. (6), it is clear that L depends on the length (L_h) and width (w) of the rectangular stub. The length of the stub should be less than a quarter wavelength. The length and width of the rectangular stub in the proposed structure is taken considering the separation between the radial section and slotted section to be greater than 0.5 mm to cancel the effect of coupling and size of the complete structure is compact. Afterwards, the value of the C_{rs1} can be calculated using Eq. (16) and hence the outer radius (r_o) from Eq. (3) by taking f_1 as 2.4 GHz keeping $\theta_r = 60^o$.

The second resonant frequency depends on L_{rs2} and C_{rs2}, which are the inductance and capacitance of the radial stub respectively. These two elements depend on the parameters of the radial stub as inner radius (r_i), outer radius (r_o) and radial angle (θ_r). As $f_2 = 5.2$ GHz is greater than f_1, the size of the radial section is small. For the resonant frequency (f_2), these parameters can be calculated by using the design equations [11,13-14] by taking $\theta_r = 40^o$. The radial angle (θ_1) for the radial section (rs2) is smaller than the angle (**α**) of the slotted radial section to keep proper separation between the two radial sections.

IV. Experimental Result

The proposed embedded filter is finally fabricated as shown in Fig. 11. Its characteristics are measured using vector network analyzer (VNA). A comparison of simulation results and experimental results are shown in Fig. 12. The experimental results are in good agreement with the simulation results.

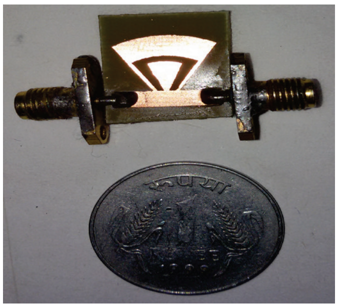

Fig. 11. Fabricated structure

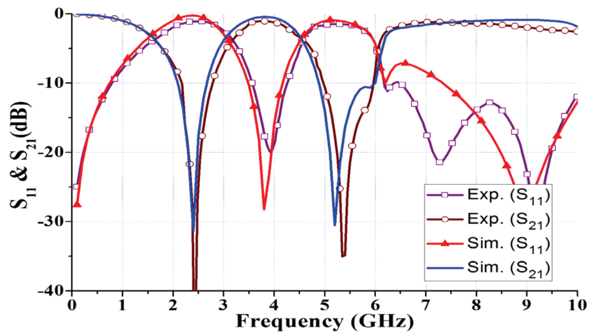

Fig. 12. Simulated and experimental result

Table III shows the comparison of proposed embedded filter with other dual bandstop filters reported in the literature.

TABLE III
COMPARISON OF PROPOSED WORK WITH PUBLISHED ARTICLES

Parameters/ Ref.	[4]	[5]	[6]	[7]	This Work
f_1/f_2 (GHz)	2.4/5.2	2.6/5.3	2.1/5.95	0.84/1.16	2.4/5.2
S_{21} (f_1/f_2) (dB)	42/44	>10/>10	>10/>10	18/49	31.2/30.1
S_{11} (f_1/f_2) (dB)	-	-	-	-	0.24/0.9
Stopband FBW (f_1/f_2) (%)	15.3/3.4 (40 dB)	61/26.8 (10 dB)	76.2/26.9 (10 dB)	22.6/16.8 (3 dB)	65.42/34.23 (3 dB)
Size (mm^2)	21×16	42×27	45×25	81.3×41.4	13.4×13.4

V. Conclusion

In this paper, a compact embedded radial dual bandstop filter is analyzed, simulated, fabricated and measured. The two stopbands are around 2.4 GHz and 5.2 GHz and can be controlled easily to achieve the specified stopband. The proposed filter offers improved passband characteristic in addition to the compactness which is achieved by embedding one radial stub inside another slotted radial stub section. An overall size reduction of 47.8 % is achieved. The proposed dual bandstop filter can be used for wireless application.

References

[1] G. Matthaei, L. Young, and E. M.T. Jones, *Microwave Filter, Impedance-matching Networks, and Coupling Structures*, Norwood, MA, Artech House, 1980.

[2] K.-S. Chin, J.-H. Yeh, and S.-H.Chao, "Compact Dual-band Bandstop Filters Using Stepped Impedance Resonators", *IEEE Microw. and Wireless Components Lett.*, vol. 17, no. 12, pp. 849–851, 2007.

[3] K.-S. Chin, J.-H. Yeh, and S.-H. Chao, "Novel Microstrip Bandstop Filters with Controllable Dual Stopbands", *Asia-Pasific Microw. Conference*, Bangkok, Thailand, 2007.

[4] F.-C. Chen, J.-M. Qiu, and Q.-X. Chu, "Dual-band Bandstop Filter Using Stub-Loaded Resonators with Sharp Rejection Characteristic", *Electronics Lett.*, vol. 49, no. 5, 2013.

[5] W. J. Feng, W. Q. Che, S. Y. Shi and Q. Xue, "Compact Dual-Wideband Bandstop Filters Based on Open-Coupled Lines and Transversal Signal-Interaction Concepts", *IET Microw. Antennas Propag.*, vol. 7, no.. 2, pp. 92–97, 2013.

[6] S. J. Xue, H. T. Zhu, W. J. Feng, and W. Q. Che, "Dual-wideband Bandstop Filter Using Transversal Signal-interaction Concept", *Electronics Lett.*, vol. 49, no. 9, 2013.

[7] W. Wang, M. Liao, Y. Wu, and Y. Liu, "Small-size High-selectivity Bandstop Filter with Coupled-line Stubs for Dual-band Applications", *Electronics Lett.*, vol. 50, no. 4, pp. 286–288, 2014.

[8] H.-K. Chiou and C.-F. Tai, "Dual-band Microstrip Bandstop filter Using Dual-mode Loop Resonator", *Electronics Lett.*, vol. 45, no. 10, 2009.

[9] S.H. Fu, and C.M. Tong, "A Novel CSRR-based Defected Ground Structure with Dual-bandgap Characteristics," *Microw. Opt. Technol. Lett.*, vol. 51, pp. 2908-2910, 2009.

[10] A. M.E. Safwa, S. Tretyakov, and A. Räisänen. "Dual Bandstop Resonator Using Combined Split Ring Resonator and Defected Ground Structure," *Microw. Opt. Technol. Lett.*, vol. 49, pp. 1249-1252, 2007.

[11] F. Giannini, R. Sorrentino, and J. Vrba, "Planar Circuit Analysis of Microstrip Radial Stub", *IEEE Trans. Microw. Theory Tech.*, vol. 32, pp. 1652–1655, 1984.

[12] H. Kwon, H. Lim, and B. Kang, "Design of 6–18 GHz Wideband Phase Shifters Using Radial Stubs", *IEEE Microw. and Wireless Components Lett.*, vol. 17, no. 3, pp. 205–207, 2007.

[13] H. A. Atwater, "Microstrip Reactive Circuit Elements", *IEEE Trans. Microw. Theory Tech.*, vol. 31, no. 6, pp. 488–491, 1983.

[14] S. L. March, "Analyzing Lossy Radial-line Stubs", *IEEE Trans. Microw. Theory Tech.*, vol. 33, pp. 269–271, 1985.

[15] K. Ma, and K. S. Yeo, "New Ultra-wide Stopband Low-pass filter Using Transformed Radial Stubs", *IEEE Trans. Microw. Theory Tech.*, vol. 59, no. 3, pp. 604–611, 2011.

[16] J.-S. Hong, and M. J. Lancaster, *Microstrip filters for RF/Microwave Applications*, New York, John Wiley & Sons Inc.,2001.